

Capacitor Voltage Estimation for Predictive Control Algorithm of Flying Capacitor Converters

Ricardo P. Aguilera and Daniel E. Quevedo
School of Electrical Engineering Computer Science
The University of Newcastle
NSW 2308, Australia

e-mails: ricardo.aguilera@studentmail.newcastle.edu.au, dquevedo@ieee.org

Abstract—Multilevel Converters have emerged as a promising alternative to traditional two level converters, especially flying capacitor converters because of the fact that this topology requires only a main dc-link voltage and presents a easy way to increase the output voltage levels by increasing the number of cells. Unfortunately, a balancing of capacitor voltage is required. Recently, predictive control algorithms have been presented in order to control not only the output current but also to achieve good performance in the balancing of the capacitor voltages. For this purpose, it is necessary to know the state of these voltages generally taking a measurement of them, therefore the number of sensors required will be increased regarding the output voltage levels desired. This paper presents an estimation of the capacitor voltages using a Discrete Kalman Filter. This algorithm is employed to determinate correctly the system state and thus provides this information to the Predictive Controller in order to determinate the best switching combination to be applied in the next sample period.

I. INTRODUCTION

Recently, the demand of higher power applications has increased considerably. In this field multilevel converters (MCs) have emerged as an important technology in comparison to their two level counterparts, not only for the high power levels than they can operate but also for the power quality than they can deliver [1], [2].

Among MCs, flying capacitor converters (FCCs) have attracted significant attention [3]. These converters are composed of multiple interconnected cells. Every cell contains two switches and one capacitor. As the number of the output voltage levels depends on the number of cell, it is easy to increase the amount of levels by adding more cells. Other important characteristic present in FCCs is the ability to contain cell faults [4] due to internal current faults decay quickly, since the associated capacitors seek voltage balance.

A disadvantage of the FCCs is that they require a balancing control of flying capacitor voltages. The dominant switching strategies utilized to synthesize the output voltage required is Phase Shifted Pulse Wide Modulation (PS-PWM) [5] which achieves the balancing of the capacitor voltages in steady state. Nevertheless, this method presents a slow dynamic in transients, e.g., a star-up condition.

Recently, predictive control strategies have been applied to power converters and multilevel converters in particular, see e.g. [6]–[10]. Advantages of using predictive control, when compared to traditional PWM methods, derive from the fact

that changing operating conditions are explicitly accounted for. Particularly in [8], a predictive control strategy for FCCs is proposed in order to control the output current and the internal capacitor voltages. This technique achieves fast response time in transients, good tracking references and low distortion in the electrical variables. The disadvantage of this method is that it is necessary to take measurements of each capacitor voltage what implies that the number of sensor required grows when the amount of cells is increased.

On the other hand, an active control and observation of capacitor voltages of a 3 cell FCC is proposed in [11]. In this work, a simplified model based on average values over one third of switch period of a PS-PWM is used to carry out a close-loop control, which selects an appropriate duty cycle to achieve a capacitor voltage tracking and output current tracking. In addition, in order to reduce the number of sensors, this model is used to estimate the capacitor voltage from output current measurement. This observer is improved applying a recursive Kalman Filter in order to take into account the current measurement noise. Moreover, to obtain a suitable capacitor voltage balance, a dc-link voltage measurement is added but the noise of this measurement is not considered.

This paper presents a capacitor voltages estimation algorithm for a flying capacitor converter using a Discrete Kalman Filter (DKF) which is possible to use in combination with, but it is not limited to, a Constraint Finite Control State Model Predictive Control strategy. Also two approaches to achieve the balancing of the capacitor voltages are considered depending of which measurement is available, the dc-link voltage or the output voltage. Even though the most usual is to have the dc-link voltage measurement, especially when the dc-link voltage is supplied by a controlled rectifier, in some case the output voltage measurement is required, for example in fault detection algorithms [4], [12].

II. FLYING CAPACITOR CONVERTER

In this section we describe the flying capacitor topology in more detail and develop a model for the system.

Figure 1 shows a schematic of a single phase three-cell flying capacitor converter. Here it is possible to see how the cells are interconnected. As mentioned above, each cell i consists of a capacitor C_i and two switching elements S_i and

\bar{S}_i which, at the same instant, cannot present the same state in order to avoid a short-circuit or an open-circuit in the cell.

The system is supplied by a dc-link voltage V_{dc} . It is important to note that the load is connected between the output point a and the middle point of the dc-link n , it is necessary to generate an alternating output current. In general, for a FCC of N -cell, the voltage that each switch has to block in an open state is given by the difference between the two adjacent capacitor voltages. To ensure that this voltage will be the same for every switch, each capacitor C_i must be charged with a voltage of iV_{dc}/N . As a result of this, a blocking voltage of V_{dc}/N will be achieved for every switch.

A. Continuous Model of Flying Capacitor Converters

As the two switches in the same cell work in complementary way, the state of this pair of switch can be represented only by the state of one of them. It can be expressed as follow:

$$S_i(t) = \begin{cases} 0 & \text{if } S_i = 0 \text{ and } \bar{S}_i = 1, \\ 1 & \text{if } S_i = 1 \text{ and } \bar{S}_i = 0. \end{cases} \quad (1)$$

for all $i \in \{1, 2, 3\}$.

Depending on which switch combination is applied, in the converter output will appear different combinations of the capacitors voltages v_{ci} and the dc-link voltage V_{dc} . Hence, the output voltage can be represented by:

$$v_{an}(t) = (S_1(t) - S_2(t))v_{c1}(t) + (S_2(t) - S_3(t))v_{c2}(t) + (S_3(t) - 1/2)V_{dc}(t). \quad (2)$$

A similar situation is presented in the capacitor currents which are defined by:

$$i_{c1}(t) = i_L(t)(S_2(t) - S_1(t)), \quad (3)$$

$$i_{c2}(t) = i_L(t)(S_3(t) - S_2(t)). \quad (4)$$

Table I shows the output voltage and capacitor currents as a function of switch states.

Finally, a simple dynamic model of the system can be developed based on elementary circuit analysis of the electrical

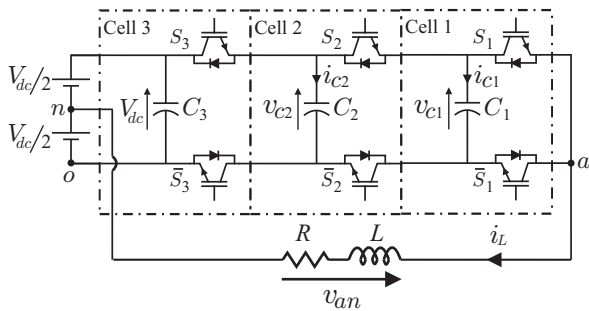


Fig. 1. Single phase FC converter.

TABLE I
SWITCH STATES AND OUTPUT VOLTAGES OF AN FCC

S_3	S_2	S_1	$v_{an}(t)$	$i_{c1}(t)$	$i_{c2}(t)$
0	0	0	$-V_{dc}(t)/2$	0	0
0	0	1	$v_{c1}(t) - V_{dc}(t)/2$	$-i_L$	0
0	1	0	$v_{c2}(t) - v_{c1}(t) - V_{dc}(t)/2$	i_L	$-i_L(t)$
0	1	1	$v_{c2}(t) - V_{dc}(t)/2$	0	$-i_L(t)$
1	0	0	$V_{dc}(t)/2 - v_{c2}(t)$	0	$i_L(t)$
1	0	1	$V_{dc}(t)/2 - v_{c2}(t) + v_{c1}(t)$	$-i_L(t)$	$i_L(t)$
1	1	0	$V_{dc}(t)/2 - v_{c1}(t)$	$i_L(t)$	0
1	1	1	$V_{dc}(t)/2$	0	0

topology shown in Fig. 1.

$$\frac{dv_{c1}(t)}{dt} = \frac{i_L(t)}{C_1}(S_2(t) - S_1(t)), \quad (5)$$

$$\frac{dv_{c2}(t)}{dt} = \frac{i_L(t)}{C_2}(S_3(t) - S_2(t)), \quad (6)$$

$$\frac{di_L(t)}{dt} = -\frac{R}{L}i_L(t) + \frac{1}{L}v_{an}(t). \quad (7)$$

B. Discrete-Time Representation

To obtain a discrete time model for the system, we first apply forward Euler approximation to the capacitor voltage equations (5) and (6). This method assumes that the capacitor current $i_{cx}(t)$ is constant within the sampled period h as it is shown in the Fig. 2-a).

$$v_{c1}[k+1] = v_{c1}[k] + \frac{h}{C_1}(S_2[k] - S_1[k])i_L[k], \quad (8)$$

$$v_{c2}[k+1] = v_{c2}[k] + \frac{h}{C_2}(S_3[k] - S_2[k])i_L[k], \quad (9)$$

The output current can be transformed into discrete time using zero order hold approximation. In this case we are assuming that the converter applies a constant load voltage $v_{an}(t)$ within the sampled period h (see Fig. 2-b)).

$$i_L[k+1] = K_a i_L[k] + K_b v_{an}[k]. \quad (10)$$

where the constant K_a and K_b are given by:

$$K_a = e^{-h\frac{R}{L}}, \quad (11)$$

$$K_b = (1 - K_a)/R. \quad (12)$$

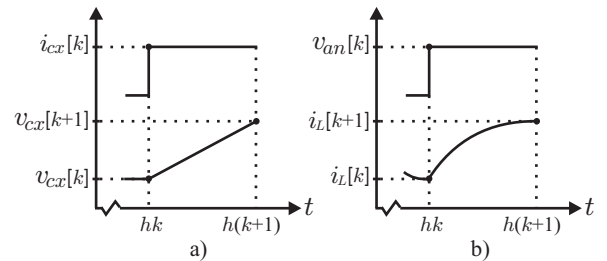


Fig. 2. Assumptions on the discretization of the model. a) constant capacitor current within the sampled period h ; b) constant load voltage within the sampled period h .

and the output voltage $v_{an}[k]$ is defined by:

$$v_{an}[k] = (S_1[k] - S_2[k])v_{c1}[k] + (S_2[k] - S_3[k])v_{c2}[k] + (S_3[k] - 1/2)V_{dc}[k]. \quad (13)$$

III. CAPACITOR VOLTAGES ESTIMATION

In this section a DKF algorithm to estimate the capacitor voltage is presented. Also two approaches are considered depending on the availability of measurements.

A. The Discrete Kalman Filter Algorithm

A Kalman Filter is a state observer for a gaussian stochastic process in which the covariance of the state estimate is minimized considering the process and measurement noises. DKF allows one to obtain the optimal estimation of the system state variables regarding the minimization of the mean square error adjusting the estimations throughout each sample time.

Firstly, the system is defined as:

$$\begin{aligned} x[k+1] &= F[k]x[k] + w[k] \\ y[k] &= C[k]x[k] + v[k] \end{aligned} \quad (14)$$

where $w[k]$ is the process noise vector and $v[k]$ is the measurement noise vector. They are considered as white gaussian noises and independents between them. It is represented by:

$$p(w[k]) \sim N(0, Q), \quad (15)$$

$$p(v[k]) \sim N(0, R). \quad (16)$$

where Q is the process noise vector and R is the measurement noise vector.

To implement the DKF, two parts can be considered, "Time update" and "Measurement update", as following:

Time update: in this stage the algorithm projects the state ahead from the current state observation to be used in the next sample time. In addition, the error covariance is also projected ahead.

- Project the state ahead

$$\hat{x}^-[k+1] = F\hat{x}[k]. \quad (17)$$

- Project the error covariance ahead

$$P^-[k+1] = FP[k]F^T + Q. \quad (18)$$

Measurement update: in this stage the algorithm calculates the current filter gain vector from the projected error covariance. With this gain and the system measurements the algorithm determines the current variable state. Finally, the update of the error covariance is obtained.

- Kalman filter gain

$$K[k] = P^-[k]C[k]^T(C[k]P^-[k]C[k]^T + R)^{-1}. \quad (19)$$

- Update estimate from measurements $y[k]$

$$\hat{y}[k] = C[k]\hat{x}^-[k], \quad (20)$$

$$\hat{x}[k] = \hat{x}^-[k] + K[k](y[k] - \hat{y}[k]). \quad (21)$$

- Update the error covariance

$$P[k] = P^-[k] - K[k]C[k]P^-[k]. \quad (22)$$

B. DKF implementation in a Flying Capacitor Converter

To implement the DKF in a FCC it is necessary to define the state variables $x[k]$, the measured variables $y[k]$ and the matrix $F[k]$ and $C[k]$. From equations (8) and (9) it is possible to see that the capacitor voltages $v_{ci}[k+1]$ can be estimated using only the output current $i_L[k]$ measurement. However, to achieve the balancing of the capacitor voltages, it is necessary to know the current value of the dc-link voltage $V_{dc}[k]$. Hence, this voltage is also considered as a state of the system. Due to the dynamic of this voltage is slow because of its high capacitance. The dc-link voltage is modeled by:

$$V_{dc}[k+1] = V_{dc}[k]. \quad (23)$$

Then, the state variable vector can be expressed by:

$$x[k] \triangleq [v_{c1}[k] \ v_{c2}[k] \ V_{dc}[k] \ i_L[k]]^T. \quad (24)$$

Considering equations (8)-(13) and (23), the matrix $F[k]$ for this system is represented by (25) as a function of switch states.

Now, it is necessary to define the variables to be measured. The first measurement considered is the output current $i_L[k]$ due to it is one of the controlled variables and with it is possible to estimate the capacitor voltages $v_{ci}[k]$. Afterwards, it is necessary to know the dc-link voltage state $V_{dc}[k]$ because of the capacitors voltages references $v_{ci}[k]$ depend on it. The easiest way to do this is to take a measurement of this voltage, especially if the converter is supplied by a controlled rectifier due to this measurement will be available. However, in other applications the output voltage v_{an} is required, e.g., fault detection algorithms. Then, to take advantage of the available measurements, we will analyze both situations.

dc-link Voltage Measurement: In this case the state variables $x[k]$ and the output variables $y[k]$ are:

$$\begin{aligned} x[k] &\triangleq [v_{c1}[k] \ v_{c2}[k] \ V_{dc}[k] \ i_L[k]]^T, \\ y[k] &\triangleq [i_L[k] \ V_{dc}[k]]^T. \end{aligned} \quad (26)$$

Then, the system is defined by:

$$\begin{aligned} x[k+1] &= F[k]x[k] + w[k] \\ y[k] &= Cx[k] + v[k] \end{aligned} \quad (27)$$

where the matrix $F[k]$ is represented by (25) and the matrix C will be:

$$C \triangleq \begin{bmatrix} 0 & 0 & 0 & 1 \\ 0 & 0 & 1 & 0 \end{bmatrix} \quad (28)$$

Here it is important to note that, unlike matrix $F[k]$, matrix C does not depend on the switching state.

Output Voltage Measurement: In this case the state variables $x[k]$ and the output variables $y[k]$ are:

$$\begin{aligned} x[k] &\triangleq [v_{c1}[k] \ v_{c2}[k] \ V_{dc}[k] \ i_L[k]]^T, \\ y[k] &\triangleq [i_L[k] \ v_{ao}[k]]^T. \end{aligned} \quad (29)$$

$$F[k] \triangleq \begin{bmatrix} 1 & 0 & 0 & \frac{h}{C_1}(S_2[k] - S_1[k]) \\ 0 & 1 & 0 & \frac{h}{C_2}(S_3[k] - S_2[k]) \\ 0 & 0 & 1 & 0 \\ K_b(S_1[k] - S_2[k]) & K_b(S_2[k] - S_3[k]) & K_b(S_3[k] - 1/2) & K_a \end{bmatrix}. \quad (25)$$

Then, the system is defined by:

$$\begin{aligned} x[k+1] &= F[k]x[k] + w[k] \\ y[k] &= C[k]x[k] + v[k] \end{aligned} \quad (30)$$

where the matrix $F[k]$ is represented by (25) and the matrix $C[k]$ will be:

$$C[k] \triangleq \begin{bmatrix} 0 & 0 & 0 & 1 \\ S_1[k] - S_2[k] & S_2[k] - S_3[k] & S_3[k] - 1/2 & 0 \end{bmatrix}. \quad (31)$$

In this case matrix $C[k]$ depends on the switching as well as $F[k]$.

IV. MODEL PREDICTIVE CONTROL OF A FLYING CAPACITOR CONVERTER

In this section, we present a model predictive control method for a FCC topology depicted in Fig. 1. The goal of this strategy is to control not only output currents but also capacitor voltages, keeping the balancing of them when disturbances in the main dc-link occur.

A. Overview

The proposed controller fits into the general framework of *Constraint Finite Control State Model Predictive Control*, as described, e.g., in [6]–[10]. This method operates in discrete time with fixed sampling period h and directly provides the switching states to be applied at the converter in order to achieve the desired tracking of the controlled variables. Consequently, no intermediate modulation stages are needed.

At each discrete time instant k , a measurement of the output current $i_L[k]$ is taken. Also it is necessary to know the capacitor voltages states $v_{ci}[k]$ and the dc-link voltage $V_{dc}[k]$. They can be obtained directly from measurements or estimated. With this information the controller will decide upon the switch states which will yield the best performance in $k+1$.

B. References Definition

As a first approach, we can consider that the dc-link voltage will remain constant. Under this condition, the capacitor voltage references will be:

$$v_{c1}^* = \frac{V_{dc}}{3} \text{ and } v_{c2}^* = \frac{2V_{dc}}{3} \quad (32)$$

these references will be constant as well. If in an operation condition the dc-link voltage is increased in $j\%$, switches S_3 and \bar{S}_3 will have to block a voltage of $3j\%$ higher than in a normal condition, due to the capacitor voltages v_{ci} will remain constant. To distribute evenly this increase, it is necessary to

raise the capacitor voltages v_{ci} in order to keep the relationship presented in (32). Then capacitor voltage references must be defined as a function of the dc-link voltage. On the other hand, the output current reference $i_L^*[k]$ will be a sinusoidal current whose magnitude will depend on the load power required. Finally, the system references are defined as following:

$$\begin{aligned} v_{c1}^*[k] &= \frac{1}{3}V_{dc}[k], \\ v_{c2}^*[k] &= \frac{2}{3}V_{dc}[k], \\ i_L^*[k] &= A \sin(\omega t). \end{aligned} \quad (33)$$

C. Optimization Criterion

The desired aim that the controller has to achieve is not only to obtain a good performance in the output current tracking, but also to keep the balancing of the capacitor voltages. To incorporate this target to the controller, we first define the error signals of the system via:

$$e[k] \triangleq \begin{bmatrix} v_{c1}[k] - v_{c1}^*[k] \\ v_{c2}[k] - v_{c2}^*[k] \\ i_L[k] - i_L^*[k] \end{bmatrix} \quad (34)$$

At each time instant k , the states of the capacitor voltages and load current are determined either by measuring or by estimating, and then they are used to minimize the following cost function:

$$J(S_1, S_2, S_3)[k] = e[k]^T P e[k] \quad (35)$$

where

$$P = \text{diag}\{\lambda_1, \lambda_2, 1\} \quad (36)$$

Here, λ_1 and λ_2 are design parameters, which allow one to trade current tracking errors versus capacitor voltage tracking errors and, thus, achieve the proposed target. The decision variables are S_1 , S_2 and S_3 , which represent the best switching combination which minimizes the cost function (35).

Finally in the Fig. 3 a block diagram of the complete strategy is presented. Here is possible to see that we can choose the measurement of either the dc-link voltage V_{dc} or the output voltage v_{an} and the output current measurement in order to estimate the state variables of the system using a DKF algorithm. Afterwards, these estimations are used as an input of the MPC algorithm which carries out the optimal switching combination which allows one to achieve the desired output current and remain the balancing of the capacitor voltages.

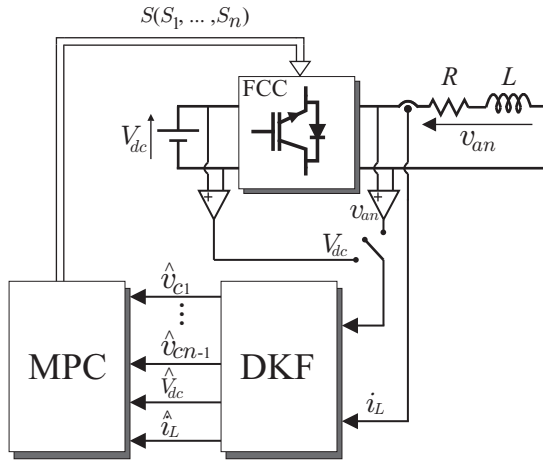


Fig. 3. Block Diagram of the proposed strategy

V. RESULTS

To verify the performance of the proposed strategy, simulation studies were carried out on a single-phase 3-cell FCC shown in Fig. 1. A main dc-link voltage of $V_{dc}=600[V]$ was used. The electrical parameters were: $C_i=100[\mu F]$, $R=20[\Omega]$ and $L=10[mH]$. The output current reference i_L^* has an amplitude of $10[A]$ and a frequency of $f_o=50[Hz]$.

These simulations consisted of implementation of the strategy proposed (see Fig. 3). Moreover, the performance of the converter operating under both approaches will be compared.

The MPC strategy is applied using a sample frequency of $f_s = 10[kHz]$. This is a reasonable sample period which allows one to implement the proposed method in a standard digital signal processor. Also the weigh factors used in the controller are $\lambda_1=\lambda_2=0.001$.

On the other hand, it is necessary to set the DKF in order to get a good performance in the estimation. We first consider a gaussian white noise which presents a variance $\sigma_i^2 = 1$ for the current measurement and a variance $\sigma_v^2 = 10$ for the voltage measurement. Also, a uniform low covariance value for the process is considered, so the variance matrix R and covariance matrix Q are:

$$R \triangleq \begin{bmatrix} 1 & 0 \\ 0 & 10 \end{bmatrix}.$$

$$Q = 0.01 \cdot I$$

Even though the real initial condition of the system considers that capacitors are completely discharged, we will define the desired steady state condition as a initial condition for the DKF. It allows one to verify the time that the estimation takes to reach the real state variables. Hence, the initial conditions for the DKF are:

$$P^- [0] = 1000 \cdot I,$$

$$\hat{x}^- [0] = [200 \ 400 \ 600 \ 0]^T.$$

In the first place, the strategy proposed using the dc-link voltage measurement is analyzed. Fig. 4 depicts the simulation result of this approach.

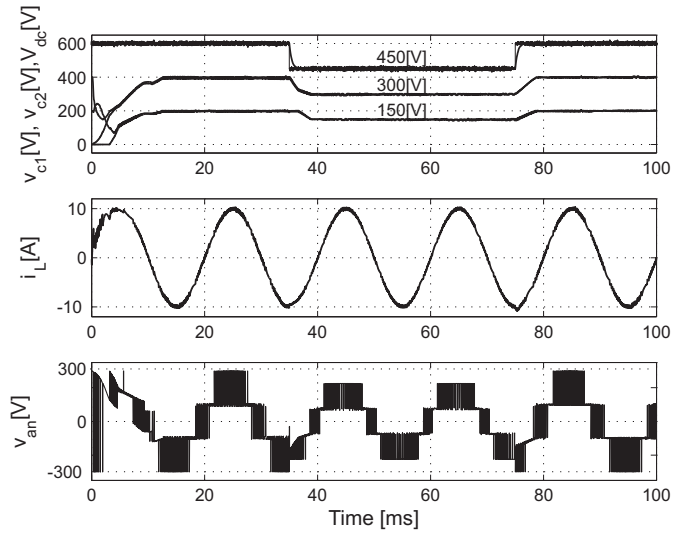


Fig. 4. Predictive control algorithm and capacitor voltages estimation considering the measurement of the output current i_L and the dc-link voltage V_{dc} : capacitors voltages v_{c1}, v_{c2} and V_{dc} ; output current i_L ; output voltage v_{an} .

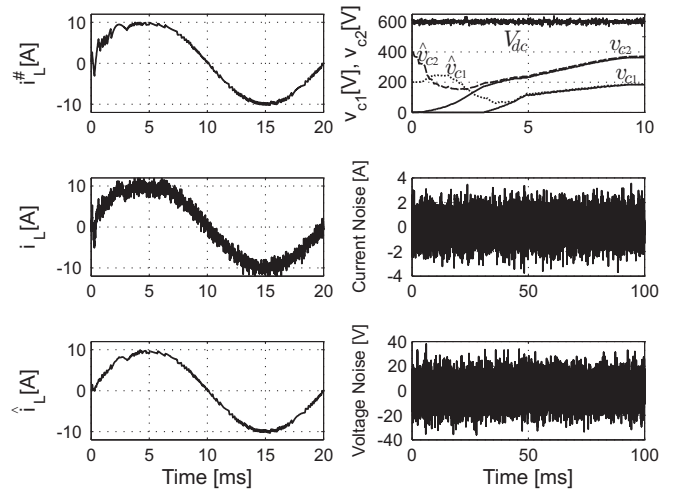


Fig. 5. Predictive control algorithm and capacitor voltages estimation considering the measurement of the output current i_L and the dc-link voltage V_{dc} . (a) output current $i_L^{\#}$; output current measurement i_L ; output current estimated \hat{i}_L . (b) capacitor voltages and their estimations; output current measurement noise; dc-link voltage measurement noise.

Here is possible to see how the controller presents a good start-up transient response reaching the desired capacitor voltage values in approximately $17[ms]$. In the instant $35[ms]$ a step down disturbance in the dc-link voltage is applied decreasing it to $450[V]$. Due to the capacitor voltage references are a function of the dc-link voltage, the controller quickly tracks the references until to reach a plateau in $v_{c1} = 150[V]$ and $v_{c2} = 300[V]$. Afterwards, the dc-link recover its original value of $600[V]$ in the instant $75[ms]$, then capacitor voltages are increased as well. It shows the controller capability to keep the balancing of the capacitor voltages.

In Fig. 5 the estimator performance is shown in more detail. Here is possible to see how the estimated current $\hat{i}_L(t)$ is

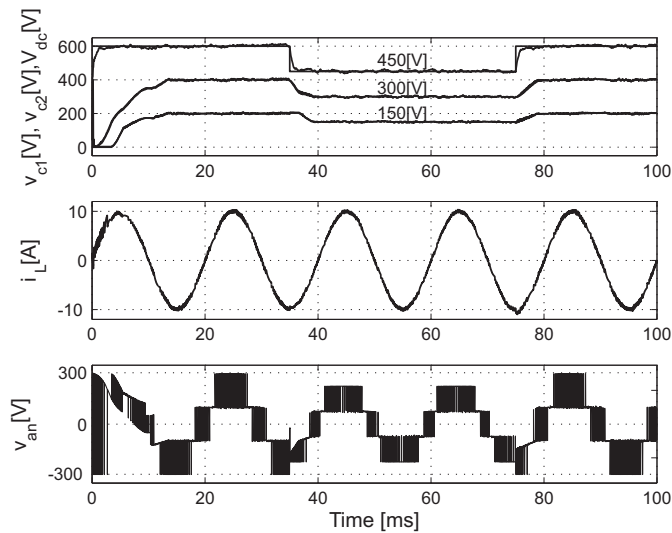


Fig. 6. Predictive control algorithm and capacitor voltages estimation considering the measurement of the output current i_L and the output voltage v_{an} : capacitors voltages v_{c1}, v_{c2} and V_{dc} ; output current i_L ; output voltage v_{an} .

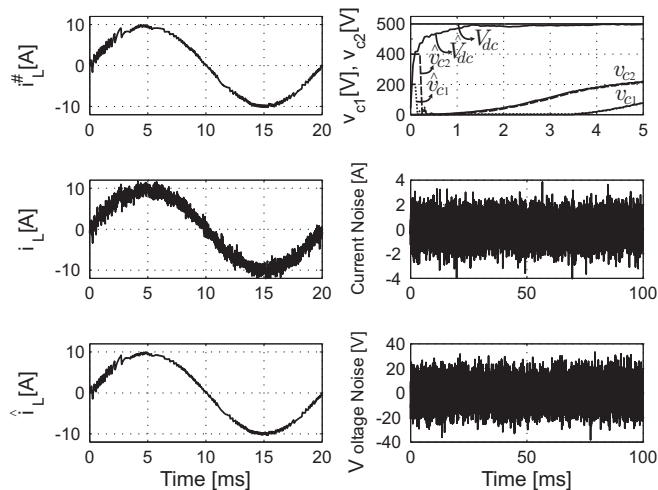


Fig. 7. Predictive control algorithm and capacitor voltages estimation considering the measurement of the output current i_L and the output voltage v_{an} . (a) output current $i_L^{\#}$; output current measurement i_L ; output current estimated \hat{i}_L . (b) capacitor voltages and their estimations; output current measurement noise; dc-link voltage measurement noise.

similar to the output current $i_L^{\#}(t)$ despite measurement noise level. Measurement of the dc-link voltage is filtered correctly by the DKF algorithm allowing to the observer to determinate appropriately the capacitor voltages states. Even though the DKF initial condition is different to the real value, after 5[ms], the estimations present a similar value than the real state.

As was explain above, capacitor voltages and dc-link voltage can be estimated considering the measurement of the output current and the output voltage. Fig. 6 depicts the result of the proposed algorithm using these measurements. Tasting condition is the same presented in the previous case using the same controller and filter parameters.

In general, the performance of this technique is similar to

use the dc-link voltage measurement with regard to the start-up transient and the balancing of the capacitor voltages. The main difference is presented in the ability to estimate the state variables. Fig. 7 shows how the capacitor voltages and dc-link estimation reaches quickly the real values. It is made in approximately 1[ms]. It is because of output voltage is a combination of the capacitor voltages and the dc-link voltage as it is shown in the Table I.

VI. CONCLUSION

An estimation of capacitor voltages for a flying capacitor converter has been proposed. This method is presented along with a predictive control strategy where both the controller and the estimator consider a no-linear model of the system. The most important benefit of this method is the good performance achieved in the tracking of the capacitor voltages and output current despite capacitor voltages are estimated. Moreover, balancing of the capacitor is achieved through either tacking a dc-link voltage measurement or estimating it from the output voltage measurement. It gives to designers a degree of freedom with regard to the measurement requirements.

REFERENCES

- [1] J. Rodriguez, S. Bernet, B. Wu, J. O. Pontt, and S. Kouro, "Multi-level voltage-source-converter topologies for industrial medium-voltage drives," *IEEE Transactions on Industrial Electronics*, vol. 54, no. 6, pp. 2930–2945, Dec. 2007.
- [2] L. G. Franquelo, J. Rodriguez, J. I. Leon, S. Kouro, R. Portillo, and M. A. M. Prats, "The age of multilevel converters arrives," *IEEE Industrial Electronics Magazine*, vol. 2, no. 2, pp. 28–39, Jun. 2008.
- [3] T. Meynard, H. Foch, P. Thomas, J. Courault, R. Jakob and M. Nahrstaedt, "Multicell converters: basic concepts and industry applications," *IEEE Transactions on Industrial Electronics*, vol. 49, no. 5, pp. 955–964, Oct. 2002.
- [4] F. R. F. F. T. M. C. Turpin, P. Baudesson, "Fault management of multicell converters," *IEEE Transactions on Industrial Electronics*, vol. 49, no. 5, pp. 988–997, Oct. 2002.
- [5] T. Meynard, M. Fadel and N. Aouda, "Modeling of multilevel converters," *IEEE Transactions on Industrial Electronics*, vol. 44, no. 3, pp. 121–128, Jun. 1997.
- [6] D. E. Quevedo, and G. C. Goodwin, "Control of EMI from switchmode power supplies via multi-step optimization," *Proc. of the 2004 American Control Conference*, Jun. 2004.
- [7] J. Rodriguez, J. Pontt, C. Silva, P. Correa, P. Lezana, P. Cortés, and U. Ammann, "Predictive current control of a voltage source inverter," *IEEE Transactions on Industrial Electronics*, vol. 54, no. 1, pp. 495–503, Feb. 2007.
- [8] E. I. Silva, B. P. McGrath, D. E. Quevedo, and G. C. Goodwin, "Predictive Control of Flying Capacitor Converter," *Proc. of the 2007 American Control Conference*, pp. 3763–3768, Jul. 2007.
- [9] R. Vargas, P. Cortés, U. Ammann, J. Rodriguez and J. Pontt, "Predictive Control of a Three-Phase Neutral-Point-Clamped Inverter," *IEEE Transactions on Industrial Electronics*, vol. 54, no. 5, pp. 2697–2705, Oct. 2007.
- [10] P. Cortes, J. Rodriguez, D. E. Quevedo, and C. Silva, "Predictive current control strategy with imposed load current spectrum," *IEEE Transactions on Power Electronics*, vol. 23, no. 2, pp. 612–618, Mar. 2008.
- [11] G. Gateau, M. Fadel, P. Maussion, R. Bensaid, and T. A. Meynard, "Multicell converters: active control and observation of flying-capacitor voltages," *IEEE Transactions on Industrial Electronics*, vol. 49, no. 5, pp. 998–1008, Oct. 2002.
- [12] R. P. Aguilera, D. E. Quevedo, T. Summers, and P. Lezana, "Predictive control algorithm robustness for achieving fault tolerance in multicell converters," *The 34th Annual Conference of the IEEE Industrial Electronics Society*, Nov. 2008.